

Local Oscillator Phase Noise Impact on M-ary Modulation Schemes



Vítor Fialho, Fernando Fortes

Abstract: This paper presents the impact of a local oscillator phase noise on digital modulation schemes based on bit error rate and error vector magnitude. The adopted methodology enables base band metrics estimation which is dependent of a specific communication standard. A generic local oscillator phase noise model is presented to evaluate the impact of different phase noise values on error vector magnitude and bit error rate. For a phase noise of -65dBc @ 1kHz the error vector magnitude changes from 7% to 12.8%. Increasing the modulation order leads to bit error rate increment for the same phase noise value.

Keywords: Phase Noise, Digital Modulation, IQ Scatter, BER, EVM.

I. INTRODUCTION

Digital communication systems are evaluated typically by base band parameters, such as bit error rate (BER) and symbol error rate (SER). Most of the communication standards use IQ scatter metrics such as error vector magnitude (EVM), to estimate the symbol sequence error percentage. These parameters give information about the communication system, however it is difficult to evaluate how BER and EVM vary depending on local oscillator phase noise and/or additive white Gaussian Noise (AWGN).

The study of a digital communication system is supported by two types of modulations schemes: M -ary phase shift keying (M -PSK) and M -ary quadrature amplitude modulation (M -QAM). Recent phase noise studies are focused on optical communications [1] or sub-THz communications [2,3]. In alternative, some authors study an iterative constellation optimization algorithm used to find new 16-QAM symbol disposal [4]. Other research strand considers orthogonal frequency division multiplexing (OFDM) with bit-interleaved coded system, where the sensitivity is obtained as a function of the 3dB phase noise for several QAM constellations [5]. The mentioned research papers present AWGN as the channel model.

This work presents the study and evaluation of local oscillator phase noise supported on base band metrics such as BER and EVM. A relation between these two parameters and a specific phase noise value allows to infer a relation with

radiofrequency (RF) and base band parameters. The presented results are supported with a MATLAB simulation model where BER and EVM are the obtained results for several M -ary modulation schemes. This paper is organized as follows: in section II it is presented the local oscillator phase noise phenomena, described in time and frequency domain. Section III presents the M -ary digital modulation techniques for M -PSK and M -QAM constellations. It is also presented the base band figure of merit: BER and EVM. In section IV it is presented the proposed model for this work. The results and discussion are presented in section V. The conclusions and the suggested future work are presented in section VI.

II. LOCAL OSCILLATOR PHASE NOISE

In Fig. 1 it is presented a sinusoidal carrier, $c(t)$, with amplitude A_c and frequency $f_c=1/T_c$. The phase noise effect is depicted in the shaded zone. Phase noise is characterized by carrier signal random phase variations. This phenomenon leads the signal zero crossing failure in multiples of $t_0+n T_c$. This uncertainty causes errors in system timing, which leads to uncertainty in the decoding of the digital signal, resulting in phase error, usually designated in the literature as jitter [6].

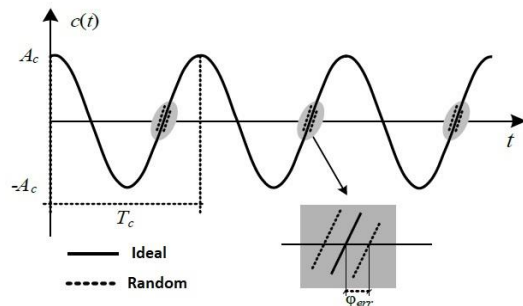


Fig. 1. Phase noise time domain: jitter

The expression of a sinusoidal carrier with phase noise is given by

$$c(t) = A_c e^{-j(2\pi f_c t + \varphi_{err}(t))} \quad (1)$$

In this paper, the amplitude noise is neglected compared to phase noise. This approximation is valid since the oscillator has a way of functioning that tends to stabilize the amplitude [6]. Thus, any disturbance in the signal amplitude converges to a constant amplitude A_c , as depicted in Fig. 1. For variations of $\varphi_{err}(t)$ smaller than 1 rad/s, expression (1) it is simplified according to expression (2), which corresponds to a narrow band phase modulation, given by a carrier centered in frequency f_c with a FM narrow band modulation.

Manuscript received on 30 September 2022 | Revised Manuscript received on 05 October 2022 | Manuscript Accepted on 15 October 2022 | Manuscript published on 30 October 2022.

* Correspondence Author (s)

Vítor Fialho*, DEETC, Instituto Superior de Engenharia de Lisboa and Centre of Technology and Systems, Lisbon, Portugal. Email: vfialho@deetc.isel.ipl.pt

Fernando Fortes, DEETC, Instituto Superior de Engenharia de Lisboa and Instituto de Telecomunicações, Lisbon, Portugal. Email: ffortes@deetc.isel.ipl.pt

© The Authors. Published by Blue Eyes Intelligence Engineering and Sciences Publication (BEIESP). This is an open access article under the CC-BY-NC-ND license <http://creativecommons.org/licenses/by-nc-nd/4.0/>



$$c(t) = A_c \cos(2\pi f_c t) - jA_c \varphi_{err}(t) \sin(2\pi f_c t) \quad (2)$$

In frequency domain, phase noise is a measure of the oscillator short-term stability. It is measured and specified as noise power relative to carrier power (P_c), in a one Hz bandwidth at a given frequency offset (Δf), as represented in Fig. 2.

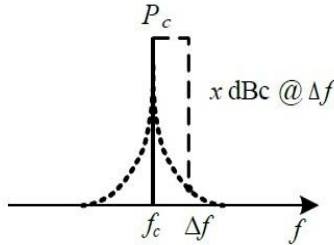


Fig. 2. Phase Noise Carrier Measurement

III. M-ARY MODULATION TECHNIQUES

Let us consider the IQ modulation concept presented in Fig. 3, composed by two base band modulating signals $m_I(t)$ and $m_Q(t)$. These signals will modulate an IQ oscillator signal given by $c_I(t)$ and $c_Q(t)$. This method is commonly designated as double side band suppressed carrier.

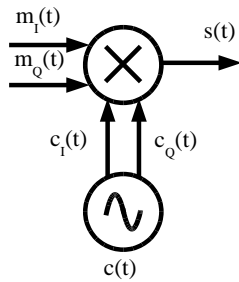


Fig. 3. IQ modulation concept

The obtained signal from the scheme presented in Fig.3 is an IQ signal, $s(t)$, given by expression (3).

$$s(t) = m_I(t) \cos(2\pi f_c t) - m_Q(t) \sin(2\pi f_c t) \quad (3)$$

Each base band signal is configured with a specific amplitude allowing the symbol geometrical placement in the IQ scatter. Thus, with correct variations of these two signals it is possible to obtain M -ary modulations, that can be M -PSK or M -QAM, as described next.

A. M-PSK

Fig. 4 presents 2-PSK, 4-PSK, Q-PSK and 8-PSK IQ scatters, derived by the general concept represented in Fig. 3. As depicted each symbol is equally distributed around the same radius, e.g., same amplitude. Thus, the only parameter that changes is the relative phase between each symbol. The binary code assigned to each symbol is compliant to Gray coding.

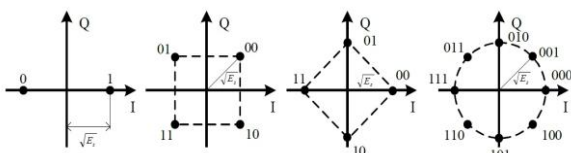


Fig. 4. 2-PSK, 4-PSK and 8-PSK IQ scatters

In Table I it is presented the IQ scatter values for the signals $m_I(t)$ and $m_Q(t)$ presented in Fig. 4. It is assumed that the carrier amplitude $A_c=1$.

Table- I: Modulating Signals Amplitude

IQ Scatter	Signal	Amplitude	Binary Code
BPSK	$m_I(t)$	1	1
	$m_Q(t)$	-1	0
QPSK	$m_I(t)$	1	00
	$m_Q(t)$	1	
	$m_I(t)$	-1	01
	$m_Q(t)$	1	
	$m_I(t)$	-1	11
	$m_Q(t)$	-1	
4-PSK	$m_I(t)$	1	00
	$m_Q(t)$	1	
	$m_I(t)$	-1	01
	$m_Q(t)$	1	
	$m_I(t)$	-1	11
	$m_Q(t)$	-1	
	$m_I(t)$	1	10
	$m_Q(t)$	-1	

B. M-QAM

In M -QAM modulation the amplitude and phase of each symbol may change according to binary coding. In Fig. 5 it is presented an example of a 16-QAM modulation. In this case it is assigned four symbols in cosine signal and other four in sine signal. Combining these two components it is obtained the IQ scatter presented in Fig. 5.

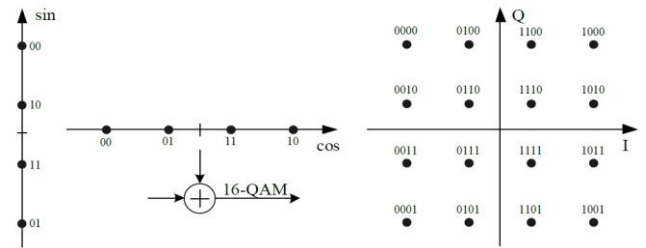


Fig. 5. 16-QAM IQ scatter: cosine and sine signal coding

Table II presents the signal configuration regarding four QAM symbols, each for one quadrant.

Table- II: Modulating Signals Amplitude

IQ Scatter	Signal	Amplitude	Binary Code
16-QAM	$m_I(t)$	1	1110
	$m_Q(t)$	1	
	$m_I(t)$	-3	0000
	$m_Q(t)$	3	
	$m_I(t)$	-1	0101
	$m_Q(t)$	-3	
	$m_I(t)$	3	1011
	$m_Q(t)$	-1	

C. Base Band Evaluation Metrics

Typical base band evaluation is supported in BER and EVM [7,8].

Expressions (4) and (5) correspond to theoretical BER for QPSK and M -QAM assuming AWGN channel and Gray coding. The relation E_b/N_0 corresponds to the quotient of bit energy and noise spectral energy density. The $erfc()$ function corresponds to the complementary error function.

$$BER_{QPSK} = 0.5 \operatorname{erfc} \sqrt{\left(\frac{E_b}{N_0}\right)} \quad (4)$$

$$BER_{MQAM} = 0.5 \left(1 - \frac{1}{\sqrt{M}}\right) \operatorname{erfc} \sqrt{\left(\frac{3k}{2(M-1)} \frac{E_b}{N_0}\right)} \quad (5)$$

According to expressions (4) and (5), for a constant value of N_0 , BER decreases when E_b increases. However, for expression (5) the BER also depends on the number of bits per symbol (k) and M . Thus, it is mandatory to establish a tradeoff between BER and data rate for the same number of symbols M . Although BER is the most common parameter in digital communication system evaluation, there are other indicators. The SER value denotes the probability of symbol error. Typically, this parameter is obtained through simulation, because, before decoding the binary codes, it is necessary to interpret the value of each symbol. Like BER, the value of the SER depends on the assignment of the binary code to the M symbols of the modulation. When the assignment of the binary code to each symbol obeys the Gray code, SER is given by expression (6).

$$BER = \frac{SER}{k} \quad (6)$$

When the binary symbol code's random, symbol decoding process can lead to errors between 1 bit to k bit in a symbol. In this case the BER is given by (7). When the assignment of the binary code is random, on average, there will be an increase of $(k+1)/2$.

$$BER = \frac{k+1}{k} \frac{SER}{2} \quad (7)$$

Like SER, EVM allows to infer the behavior of the digital communication system, however this parameter is dependent on the constellation symbol disposal of the received symbols in relation to the expected (ideal) symbols. A decoded symbol, $s_{RX}[n]$, has an error (distance) with respect to the expected symbol (ideal), $s_{TX}[n]$. It must be considered that this error does not imply the existence of a bit error, but rather a dispersion of the decoded symbols around the ideal symbol, as shown in Fig. 6. The representation is carried out between a received symbol - distorted - (+) with respect to the ideal symbol (+). The P_{err} and P_s variables corresponds to the error and signal strength, respectively. The value of $(P_{err})^{1/2}$ corresponds the Euclidean distance between the symbols.

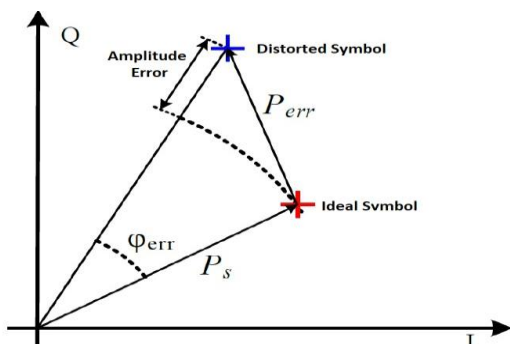


Fig. 6. IQ ideal and distorted symbol representation

Relating the parameters presented in Fig. 6, to N transmitted symbols of the constellation and normalizing to ideal signal average power it is obtained the expression (8).

$$EVM = \sqrt{\frac{\frac{1}{N} \sum_{n=1}^N (s_{RX}[n] - s_{TX}[n])^2}{\frac{1}{N} \sum_{n=1}^N (s_{TX}[n])^2}} \quad (8)$$

Therefore, EVM corresponds to the ratio between the average normalized voltage error and the average signal voltage. Thus, the value of this relation becomes independent of the modulation order, that is, of the value of M .

IV. PROPOSED MODEL FOR DIGITAL COMMUNICATIONS SYSTEM WITH PHASE NOISE

In Fig. 7 it is presented the proposed model for evaluating the oscillator phase noise used in digital communications. This model is composed by several building blocks that are described next. The binary source generates a uniform distributed sequence number of bits. The obtained sequence is coded in M -ary modulation (M -PSK or M -QAM) by the modulator block. The obtained symbol sequence is applied to a square-root raised cosine filter with configurable roll-off factor. The sampled signal is applied to a AWGN channel and phase noise model. Phase noise is given in dBc for a specific carrier offset, as described in section II Fig. 2. The receiver is composed by a square-root raised cosine filter that processes the samples from the channel and returns the received symbols. Comparing the ideal and received (distorted) symbols, EVM is obtained according with expression (8). After this process, the obtained symbols are demodulated and decoded by the demodulator block. Comparing the transmitted and received binary sequence it is obtained the simulation BER.

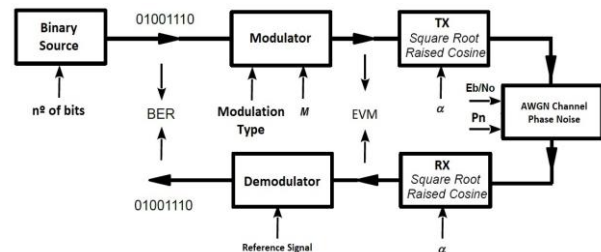


Fig. 7. Local Oscillator Phase Noise Model

To evaluate the influence of each impairment in the M -PSK and M -QAM modulation schemes, it is presented the impact AWGN and phase noise in separate scenarios and finally the global impact. Table III presents the simulation parameters used in this model. The obtained results are presented in the following subsections.

Table- III: Simulation Parameters

Number of bits	$N=1$ Mbit
Raised Cosine	Roll off = 0.25 Number of samples/symbol = 10 Delay = 10 samples
E_b/N_0	15 dB
Phase Noise	-65 dBc @ 1 kHz

A. Additive White Gaussian Noise - AWGN

Fig. 8, Fig. 9 and Fig. 10 present the Q-PSK, 8-PSK and 16-QAM IQ scatters, respectively, for the simulation parameters presented in Table III, corresponding to AWGN. For each IQ scatter it is presented the EVM value.

As depicted, the EVM is similar in all modulation schemes (11 %). This validates the expression (8), which denotes that EVM is an independent parameter regarding to the type of modulation and its order (number of symbols - M)

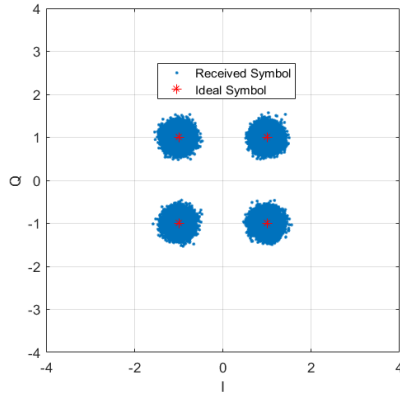


Fig. 8. QPSK – EVM=11.6% ; BER=n.a.

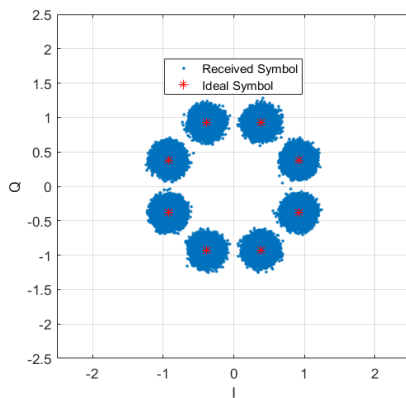


Fig. 9. 8-PSK – EVM=11.2% ; BER=n.a.

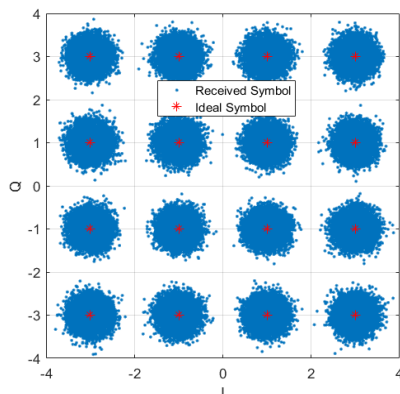


Fig. 10. 16QAM - EVM=11.9% ; BER=n.a.

B. Phase Noise

Fig. 11, Fig. 12 and Fig. 13, denote the impact of local oscillator phase noise on the decoded symbols. In this case the AWGN is not considered. The symbols on IQ scatter presents a very characteristic disposal, like an arc of circumference, denoting only the phase error.

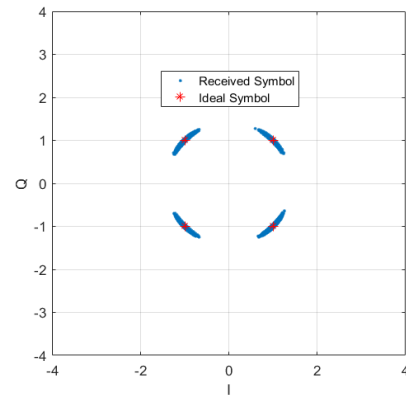


Fig. 11. QPSK – EVM=7.2% ; BER=n.a.

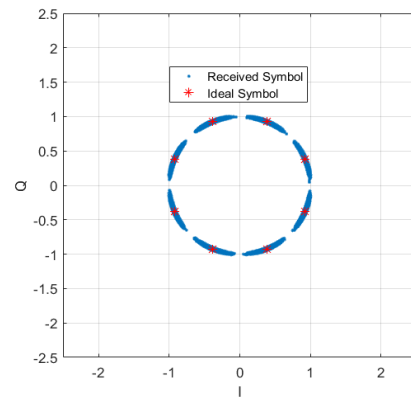


Fig. 12. 8PSK – EVM=7.2% ; BER=n.a.

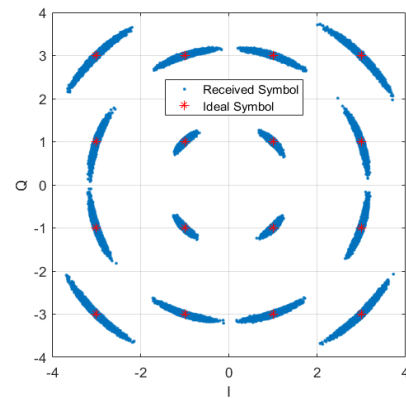


Fig. 13. 16QAM – EVM=7.4% ; BER=n.a.

C. AWGN and Phase Noise

Fig. 14, Fig. 15 and Fig. 16 present the IQ scatter for $E_b/N_0 = 15$ dB and phase noise of -65 dBc @ 10 kHz. As depicted the symbols disposal denotes a typical phase noise influence with AWGN channel. This characteristic leads to the EVM increment comparatively to the results presented in subsection IV A and IV B. However, for different modulation schemes, EVM is similar, but the BER increases with the constellation order.

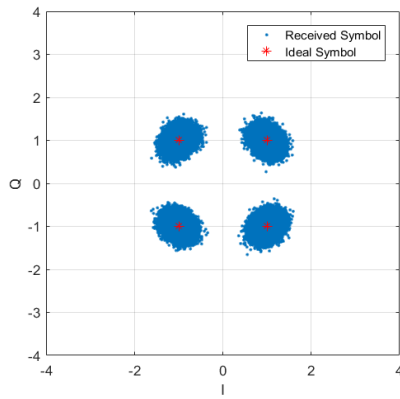


Fig. 14. Q-PSK – EVM=12.5% ; BER=n.a.

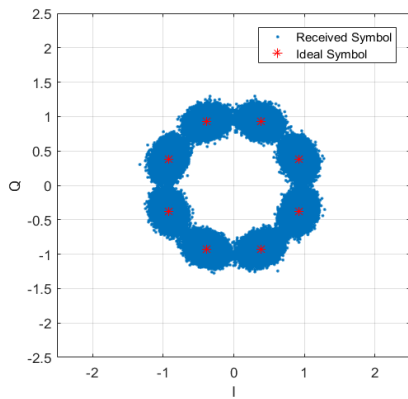


Fig. 15. 8-PSK – EVM=12.6% ; BER=4.6e-5

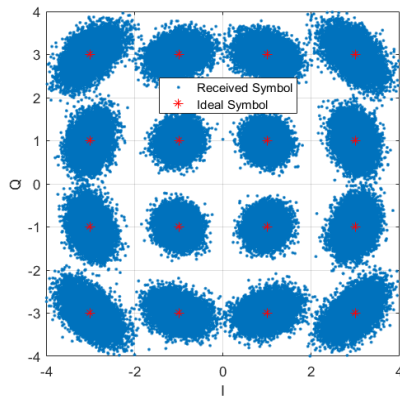


Fig. 16. 16-QAM – EVM=12.8% ; BER=1.45e-4

Since the number of bits used for all the preformed simulation is 1Mbit the simulation BER is limited to 1e-6. In these cases, the simulation BER value is not available (n.a.).

V. RESULTS AND DISCUSSION

In Fig. 17 it is presented the BER variation for Q-PSK, 16-QAM and 64-QAM under the effect of AWGN for sweep of Eb/No from 0dB to 20dB, represented by the lines with number 1. BER values correspondent to AWGN sweep with phase noise of -65dBc@10kHz are represented with lines number 2. Finally, lines designated by number 3, represent AWGN with phase noise of -60dBc@10kHz.

As depicted, for Eb/No values below 5 dB, BER values are dependent only of AWGN effect. However, for Eb/No values

above 6dB, phase noise impact is higher than AWGN, leading to an increase of BER.

As an example, for Eb/No=13dB, 64-QAM with AWGN has a lower BER value comparing with 16-QAM with phase noise of -60dBc@10kHz.

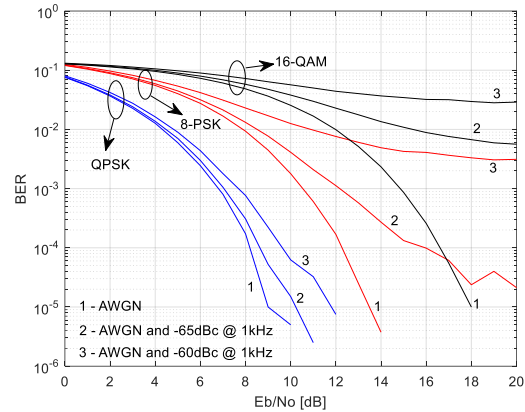


Fig. 17. BER variation with AWGN and phase noise

In Fig. 18 it is presented the EVM variation for three different simulation scenarios. As depicted the increase of phase noise value will lead to an increase of EVM. However, and unlike the BER variation, EVM is always higher in presence of phase noise, for any value of Eb/No, comparing with the reference values obtained only with AWGN channel.

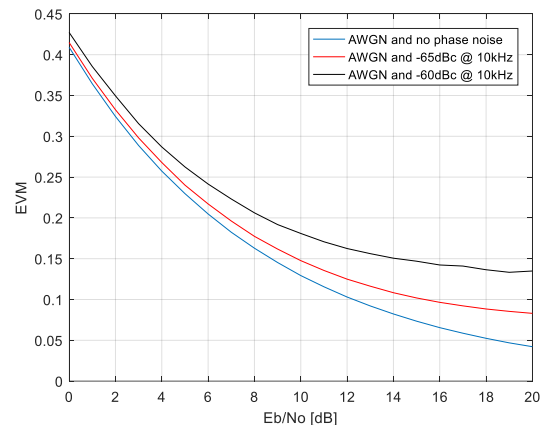


Fig. 18. M-QAM BER with AWGN and phase noise

VI. CONCLUSIONS AND FUTURE WORK

This work presents the local oscillator phase noise impact on M-ary modulation. The evaluation metrics are supported by BER and EVM. These metrics are useful since they provide the error rate and the symbol distortion of a specific modulation under a specific Eb/No. For Eb/No lower than 5dB AWGN is predominant in relation to phase noise. 16-QAM and 64-QAM modulation schemes are more sensitive to phase noise than Q-PSK, for the same values.

For higher modulation order, the phase noise impact on BER is more relevant for Eb/No higher than 12dB with a phase noise of -60dBc @ 10kHz. In this case it is preferable to use 64-QAM with AWGN rather than 16-QAM with phase noise.

The EVM itself do not provide enough information if the obtained values are consequence of a specific noise. Thus, it is necessary to verify the IQ scatter to verify the predominant noise. For future work it is proposed the study of phase noise with different values within a specific bandwidth.

REFERENCES

1. Y. Xie, P. Zhou, Z. Jiang, Z. Zhou and N. Li, "Wideband Microwave Phase Noise Analyzer Based on All-Optical Microwave Signal Processing," in IEEE Photonics Journal, vol. 14, no. 4, pp. 1-6, Aug. 2022, Art no. 5538706, doi: 10.1109/JPHOT.2022.3184596. [[CrossRef](#)]
2. A. N. Uwaechia and N. M. Mahyuddin, "A Comprehensive Survey on Millimeter Wave Communications for Fifth-Generation Wireless Networks: Feasibility and Challenges," in IEEE Access, vol. 8, pp. 62367-62414, 2020, doi: 10.1109/ACCESS.2020.2984204. [[CrossRef](#)]
3. F. Li, H. Zhang and X. Luo, "Joint Cancellation of Phase Noise and NB-IoT Interference in OFDM System," in IEEE Wireless Communications Letters, vol. 10, no. 2, pp. 436-440, Feb. 2021, doi: 10.1109/LWC.2020.3034461. [[CrossRef](#)]
4. T. Pfau, X. Liu and S. Chandrasekhar, "Optimization of 16-ary Quadrature Amplitude Modulation constellations for phase noise impaired channels," 2011, 37th European Conference and Exhibition on Optical Communication, 2011, pp. 1-3. [[CrossRef](#)]
5. Petrovic D. et al, "Phase Noise Influence on Bit Error Rate, Cut-off Rate and Capacity of MQAM OFDM Signaling", In Proc. Intl. OFDM Workshop of M-QAM OFDM Signaling (InOWo), 2002
6. Lee T. H.; Hajimiri A., "Oscillator Phase Noise: A Tutorial", IEEE Journal of Solid-State Circuits, vol. 35, no. 3 , pp. 326 - 336, Mar. 2000 [[CrossRef](#)]
7. Zareian, H.; Vakili, V.T., "Analytical BER Performance of M-QAM-OFDM Systems in the Presence of IQ Imbalance", IEEE IFIP International Conference on Wireless and Optical Communications Networks, pp. 1-5, Jul. 2007 [[CrossRef](#)]
8. Dusza, B.; Daniel, K.; Wietfeld, C., "Error Vector Magnitude Measurement Accuracy and Impact on Spectrum Flatness Behavior for OFDM-based WiMAX and LTE Systems", IEEE International Conference on Wireless Communications, Networking and Mobile Computing, vol. n.d., no. n.d. , pp. 1-4, Oct. 2009 [[CrossRef](#)]

AUTHORS PROFILE



Vítor Fialho, BsC, MsC, PhD. He received the MsC degree in 2008 from Instituto Superior Técnico (University of Lisbon) and PhD in 2017 by Faculdade de Ciências e Tecnologia (New University of Lisbon). Since 2009 he is a member of the teaching staff at Instituto Superior de Engenharia de Lisboa, Portugal. His research interests are RFIC design and RF transceiver characterization, Signal Processing and Internet of Things.



Fernando Fortes, BsC, MsC, PhD. He received BsC from Instituto Superior de Engenharia de Lisboa in 1992, MsC and PhD in 2001 from Instituto Superior Técnico, Portugal. He is an assistant professor with 20 year experience currently teaching at Instituto Superior de Engenharia de Lisboa, Portugal. His research interests

include analog and digital electronics, RF electronics, RFIC design and characterization